Magnetoassociation of a Feshbach molecule and spin-orbit interaction between the ground and electronically excited states

Yosuke Takasu, Yoshiaki Fukushima, Yusuke Nakamura, and Yoshiro Takahashi

Phys. Rev. A **96**, 023602 — Published 1 August 2017

DOI: 10.1103/PhysRevA.96.023602

Magneto-association of Feshbach molecule and spin-orbit interaction between the ground and electronically excited states

Yosuke Takasu, Yoshiaki Fukushima, Yusuke Nakamura, and Yoshiro Takahashi
Department of Physics, Graduate School of Science, Kyoto University, Kyoto 606-8502, Japan
(Dated: June 26, 2017)

By preparing a cold atom ensemble of mixtures of the ground $^1S_0$ and metastable $^3P_2$ states of ytterbium atoms ^{171}Yb, we successfully associate a Feshbach molecule $^{171}Yb_2$, with one ^{171}Yb atom in its electronically excited state and another one in the ground state, by sweeping a magnetic field across a Feshbach resonance. The atom-molecule conversion efficiency reached about 50 %, confirmed by a separate image of atoms and molecules with a Stern-Gerlach effect and an atom loss measurement. In addition, we successfully implement a spin-orbit coupling with a one-photon process between the $^3P_2$ (pseudo-spin up) and ground $^1S_0$ (pseudo-spin down) states of a Yb atom. As a benchmark, we observe a spin-momentum locking behavior at a large Rabi frequency. The achieved successful production of Feshbach molecules, along with the implementation of spin-orbital coupling between the $^1S_0$ and $^3P_2$ states, provides an important step towards the study of a topological superfluid.

I. INTRODUCTION

High controllability over various experimental parameters lies at the heart of recent remarkable advances in the study of ultracold atomic gases. Tuning the interaction between atoms with Feshbach resonances [1] is undoubtedly an fascinating aspect of this system. One of the important applications of a Feshbach resonance is a successful creation of an ultracold molecule with very small binding energies, a Feshbach molecule, by adiabatically sweeping a magnetic field across a resonance. A Feshbach molecule plays a key role in many studies such as the crossover between a Bose-Einstein Condensate (BEC) and a Bardeen-Cooper-Schriefer superfluid [2, 3], the initial step to form an ultracold, rovibronic ground state of (polar) molecules using stimulated-Raman adiabatic passage method [4–7], and so on.

The observation of Feshbach resonances was limited to those between two electronically ground state atoms until quite recent reports of Feshbach resonances between the ground $^1S_0$ state and the metastable $^3P_2$ [8, 9] and $^3P_0$ [10–12] states of two-electron atoms of ytterbium (Yb). Differently from the cases of the hyperfine-interaction-induced Feshbach resonances in alkali atoms[13], the collision between the ground and metastable states of Yb atoms is resonantly enhanced by an anisotropic electrostatic interaction or spin exchange interaction, resulting in narrow and broad Feshbach resonances.

In addition, the existence of this novel Feshbach resonance between the ground and optically excited state offers an intriguing possibility for study of Majorana fermions in a topological $p-$wave superfluid which attracts much attention from fundamental interests to applications such as quantum computing [14]. One promising approach to realize a topological $p-$wave superfluid with cold atoms is the implementation of a spin-orbital coupling (SOC) [15] to an $s-$wave fermionic superfluid, proposed in [16, 17]. While the implementation of SOC into ^{40}K [18] and ^{6}Li [19] via a Raman transition has been reported, however, a serious heating effect due to a photon scattering through intermediate states involved in the Raman process was also observed [18, 19], which has prevented the successful formation of a fermionic superfluid with SOC so far. Therefore alternative routes to implement SOC on cold atom system with interaction control are desired, and in fact, several schemes are proposed to overcome this difficulty [20–22]. One unique strategy is to use a single photon process to implement SOC between the ground and optically excited states [15, 23, 24]. An atomic system of the ground $^1S_0$ and long-lived metastable ^3P states with an $s-$wave Feshbach resonance, therefore, offers an ideal playground for exploring this novel possibility. Towards this goal, the creation of Feshbach molecules by controlling an atomic interaction between the $^1S_0$ and long-lived metastable ^3P states and implementation of SOC between these states may be a first step for the study of fermionic superfluid with SOC.

Here in this paper, we report a successful creation of a large number of Feshbach molecules between electronically excited $^3P_2$ and ground $^1S_0$ states of fermions ^{171}Yb by a magnetic-field sweep across a broad Feshbach resonance at 6.6 Gauss. By preparing a cold atom ensemble of mixtures of the ground $^1S_0$ and metastable $^3P_2$ states, the atom-molecule conversion efficiency reached about 50 %, confirmed by a separate image of atoms and molecules with a Stern-Gerlach effect. In addition, another important ingredient of SOC is also successfully demonstrated with a one-photon process between the electronically excited $^3P_2$ and ground $^1S_0$ states of Yb. As a benchmark, we observe a spin-momentum locking behavior at a large Rabi frequency. The achieved successful production of Feshbach molecules for this system, along with the implementation of SOC between the $^1S_0$ and $^3P_2$ states, provides an important step towards the study of topological superfluid. We note that a different technique of a ultranarrow photoassociation resonance between the $^1S_0$ state and $^3P_2$ states of Yb atoms was recently used for the coherent atom-molecule conversion in an optical lattice [9], which complements the presently demonstrated work.

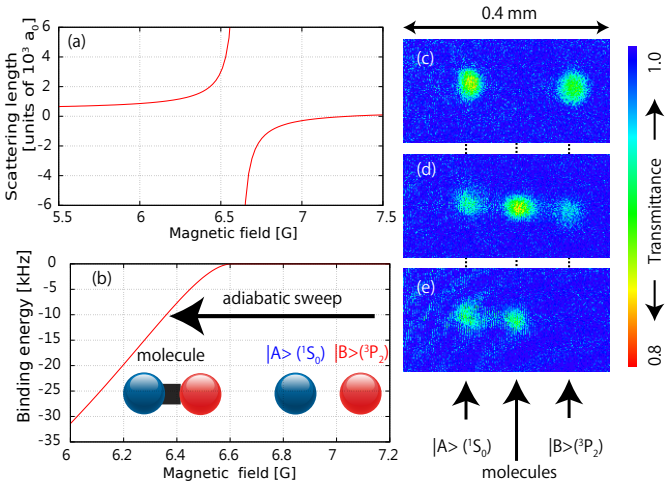

FIG. 1. Magneto-association of Feshbach molecules and the detection with a Stern-Gerlach technique. (a) scattering length as a function of a magnetic field calculated using the parameters taken from Ref [9]. A narrow resonance at 6 G is omitted in this figure. (b) binding energy of molecules as a function of a magnetic field. Note that the binding energy E_b is calculated from the scattering length a by the universal relation $E_b = \hbar^2/(ma^2)$. A narrow resonance at 6 G is also omitted in this figure. Feshbach molecules are associated by an adiabatic sweep of a magnetic field from 7.0 G to 6.2 G. (c) absorption imaging of $|A\rangle$ and $|B\rangle$ atoms before a magnetic field sweep. The TOF time is 10 ms. (d) absorption imaging of $|A\rangle$ atoms, $|B\rangle$ atoms and molecules after a magnetic field sweep from 7 G to 6.2 G. (e) absorption imaging of of $|A\rangle$ atoms and $^1S_0$ component of molecules after a magnetic field sweep from 7 G to 6.2 G.

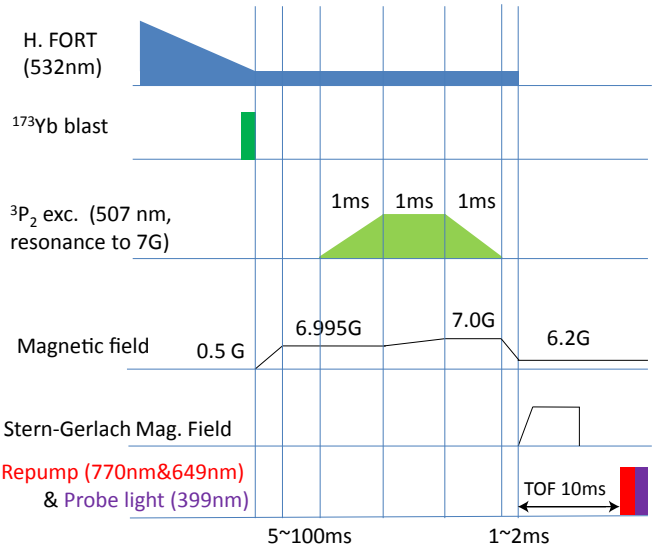

FIG. 2. Time sequence for magneto-association of Feshbach molecules and the detection with a Stern-Gerlach technique. See text for detail.

II. CREATION OF FESHBACH MOLECULES BY ADIABATIC ASSOCIATION

We first describe a successful formation of a Feshbach molecule of $^{171}Yb_2$ which consists of the ground state $^1S_0$ m_F=+1/2($\equiv |A\rangle$) and electronically excited state $^3P_2$ F=3/2, m_F=−3/2($\equiv |B\rangle$). Our experiment exploits a relatively broad Feshbach resonance around 6.6 Gauss recently observed between $|A\rangle$ and $|B\rangle$ [9] (see also Fig. 1 (a)).

Here we mention the stability of the states. The radiative lifetime of the $^3P_2$ state is about 15 seconds, which is long enough for most experiments. However, the atoms in the $^3P_2$ state suffers from a photon scattering due to the light for the optical lattice and trap, which transfers the atoms from the $^3P_2$ to $^1S_0$ states, which effectively shortens the lifetime to about 3 s at our experimental condition. For two polarized $|B\rangle$ states of ^{171}Yb atoms, the $s-$wave collision channel is inhibited by the Pauli exclusion principle. The dominant loss process is, therefore, the inelastic collision between $|A\rangle$ and $|B\rangle$, which is induced by the fine-structure-changing and principal quantum number changing collisions. This inelastic two-body loss will be enhanced near the Feshbach resonance. Note that a Zeeman-state-changing-collision is absent because of the lowest Zeeman energy of the $|B\rangle$ state.

Our experiment starts from a creation of an ultracold sample of $|A\rangle$ in a harmonic trap, by performing sympathetic cooling of ^{171}Yb with ^{173}Yb in almost the same way as in Ref. [25]. The experimental procedure after preparation of cold atoms is shown in Fig. 2. After the sympathetic evaporative cooling, we remove the remaining ^{173}Yb atoms, which results in a pure atom cloud of ^{171}Yb with a typical atom number of about 10^4 and temperature of about 25 nK, corresponding to about 0.2 times Fermi temperature T_F in a harmonic trap with trap frequencies of $(\omega_x, \omega_y, \omega_z) = 2\pi\times$ (150 Hz, 26 Hz, 140 Hz).

We then apply an excitation light beam resonant to the $|A\rangle$ -$|B\rangle$ transition of ^{171}Yb at the BCS side of the Feshbach resonance. Note that this excitation is forbidden by an electric-dipole transition but is allowed by a magnetic quadrupole transition, which couples the states with magnetic quantum number difference by 2. A coherent, adiabatic half excitation scheme [26] is used to prepare a mixture of almost equal populations of $|A\rangle$ and $|B\rangle$ states. This is done by sweeping a magnetic field around about 7 G while the frequency of the excitation laser is kept constant. A magnetic field is then swept to 6.2 G, resulting in the association of Feshbach molecules.

We note that we take special cares to obtain as cold ultracold mixture of the $|A\rangle$ and $|B\rangle$ states as possible in our setup. To optimize the sympathetic evaporative cooling, we suppress a three-body recombination loss by using only a single component of ^{173}Yb and a single component ^{171}Yb ($|A\rangle$). In addition, in order to remove ^{173}Yb atoms, we coherently excite ^{173}Yb atoms to the $^3P_2$ state and we force ^{173}Yb atoms in the $^3P_2$ state to escape from a trap by applying a magnetic field gradient, instead of blasting the atoms using the resonant light of the $^1S_0$ -$^1P_1$ or $^1S_0$ -$^3P_1$ transitions. In this way we suppress a small but finite heating effect associated with the collision with heated ^{173}Yb atoms.

We directly observe the created Feshbach molecules with

absorption imaging with a Stern-Gerlach technique. By turning off the confining trap, we release atoms and molecules to freely expand while a horizontal magnetic field gradient $B' = \delta B/\delta x$ is simultaneously turned on during a time denoted by $t_{\rm SG}$. Typically B' is 4.5 G/cm and $t_{\rm SG}$ is 9.5 ms. The magnetic force exerted during $t_{\rm SG}$ on an atom or a molecule with a magnetic moment μ is given by $F = \mu B'$. Equation of motion during TOF is described as

$$m\frac{d^2x}{dt^2} = \begin{cases} \mu B' & (0 < t < t_{\rm SG}) \\ 0 & (\text{otherwise}) \end{cases} \quad (1)$$

where m is a mass of ^{171}Yb atom. Equation (1) is easily solved (see Supplementary Material) and a spatial displacement due to the magnetic force $x_{\rm SG}$ is given by

$$x_{\rm SG} = \frac{1}{2}\frac{\mu B'}{m} t_{\rm SG}\,(2t_{\rm TOF} - t_{\rm SG})\,, \quad (2)$$

where $t_{\rm TOF}$ is a time-of-flight (TOF) time, which we typically take as 10 ms.

The magnetic moment $\mu_{\rm S}$ of the $|A\rangle$ state originates solely from the small nuclear magnetic moment $\mu_{\rm S}$ is $h \times 0.5$ kHz / Gauss, where h is the Planck constant. In contrast, the magnetic moment $\mu_{\rm P}$ of the $|B\rangle$ state is as large as about $h\times(-3.78)$ MHz / Gauss. For the Feshbach molecules, the expected magnetic moment $\mu_{\rm mol}$ is

$$\mu_{\rm mol} = \mu_{\rm S} + \mu_{\rm P} - \frac{dE_b}{dB}, \quad (3)$$

where E_b is the binding energy of molecules and B is an external magnetic field. From the measured binding energies of ^{171}Yb molecules ([9]) we obtain $\mu_{\rm mol} \sim \mu_{\rm P}$. Since the mass of Feshbach molecules is twice of the atoms and the magnetic moment of the ^{1}S$_0$ state is very small, Feshbach molecules are expected to appear at almost a halfway between the ^{1}S$_0$ and ^{3}P$_2$ atoms after TOF and can be detected separately.

Figure 1 (c)-(e) show absorption images of atoms and molecules. Associated Feshbach molecules as well as remained atoms are clearly shown in Fig 1 (d,e). Note that, since the binding energy of Feshbach molecules is less than 100 kHz [9], much smaller than the natural linewidths of imaging and repumping transitions of 29 MHz and 11 MHz, therefore, imaging and repumping light dissociate Feshbach molecules into isolated atoms which are detected in our method. In contrast, when a magnetic field is not swept and kept at 7.0 G, no molecules are observed (Fig 1 (c)). In the absence of the repumping light, we can measure atoms and molecules in the ^{1}S$_0$ state (Fig 1 (e)). These measurements provide clear evidence that we successfully associate Feshbach molecules by a magnetic field sweep.

From the absorption imaging data, we can evaluate a conversion probability from the atoms to the molecules. For this purpose it is better to count the numbers of the ^{1}S$_0$ state in the Feshbach molecule and unassociated atoms, which are free from the repumping efficiency of the ^{3}P$_2$ state. The number of the ^{1}S$_0$ atoms associated with Feshbach molecules $N_S^{\rm mol}$ and the number of the atoms of the unassociated ^{1}S$_0$ atoms $N_S^{\rm atom}$ are 3.5×10^3 and 3.0×10^3, respectively, from Fig. 1, which results in a conversion probability $N_{\rm mol}/(N_{\rm atom} + N_{\rm mol})$ of about 54 %.

Provided that the association is performed well adiabatically, the conversion probability can be used as a measure of the atom temperature [27, 28]. The previous result [27] shows that the conversion probability is about 54 % when the atom temperature is 0.4 T_F, close to the temperature of 0.37 T_F estimated from the TOF image shown in Fig. 1 (c). However, this is higher than the initial temperature of 0.2 T_F just before the ^{3}P$_2$ excitation, which indicates the heating of an atom cloud during the ^{3}P$_2$ excitation. We may well think that the heating is induced by hole creation in the atom cloud as a result of the ^{3}P$_2$ excitation from the deeply degenerate Fermi gas in the ^{1}S$_0$ state, as is discussed in [29]. This consideration suggests us to prepare an ultracold sample of m_F=+1/2(= $|A\rangle$) and m_F=−1/2(≡ $|C\rangle$) mixture of the ground ^{1}S$_0$ state, and then transfer only the $|C\rangle$ state into the ^{3}P$_2$ $|B\rangle$ state. At the expense of the merit that this scheme does not suffer from the hole-creation heating effect, we need to optimize the sympathetic evaporative cooling to minimize a three-body recombination for the $|A\rangle$ and $|C\rangle$ mixture of ^{171}Yb and single component ^{173}Yb, which is a future work in our research.

III. LOSS MEASUREMENT AFTER SWEEPING ACROSS FESHBACH RESONANCE

We also perform a high-sensitive fluorescence measurement of atoms with a magneto-optical trap (MOT) using the dipole-allowed ^{1}S$_0$ -^{1}P$_1$ transition [8, 9] in order to measure the atom loss possibly associated with the creation of Feshbach molecules. Note that we cannot distinguish molecules from atoms in the florescence imaging with a MOT, in contrast to the absorption imaging with the Stern-Gerlach method previously mentioned. The creation of Feshbach molecules is, instead, expected to be identified as a rapid loss of atoms remaining after the magnetic field sweep. We separately measure the number of atoms in the ^{1}S$_0$ and the ^{3}P$_2$ states by appropriately combining repumping and blast laser beams. Again we note that imaging and repumping light dissociate Feshbach molecules into isolated atoms which are detected in this method.

The time sequence is shown in Fig. 3. We prepare an unpolarized sample of ^{171}Yb in the ^{1}S$_0$ state. Then we excite almost all $|C\rangle$ atoms into the ^{3}P$_2$ state (F=3/2, m_F=−3/2) (= $|B\rangle$) at 7.47 G, which is above the resonant magnetic field of the Feshbach resonance and the scattering length is almost zero. In order to avoid the recoil heating associated with the ^{3}P$_2$ excitation, we exploit the recoil-free excitation using an optical lattice. After trapping unpolarized ^{171}Yb atoms, we linearly increase a depth of a three-dimensional optical lattice from zero to 15 E_R^{532} in 200 ms, where E_R^{532} is the photon recoil energy of 532-nm light. The excitation light resonant to the $|A\rangle$ -$|B\rangle$ transition at 7.47 G is then turned on and has the intensity of 5.2 W/cm^2. The magnetic field is changed from 7.474 G to 7.466 G in 1 ms, while the frequency and intensity of excitation laser kept constant. After we excite atoms in the

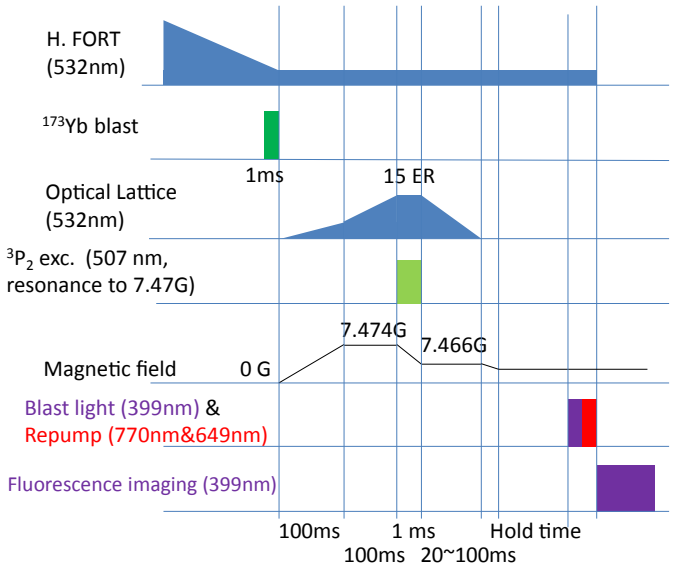

FIG. 3. Time sequence for magneto-association of Feshbach molecules and the detection with a MOT. See text for detail.

$|C\rangle$ state into the $|B\rangle$ state, we decrease the lattice depth from 15 E_R^{532} to zero in typically 20~100 ms.

Figure 4 shows the numbers of the atoms in the $^1S_0$ and $^3P_2$ states as a function of holding time after a linear magnetic field sweep from 7.466 G to final magnetic fields of (a) 7.5 G, (b) 6.6 G, (c) 6.2 G, and (d) 5.5 G in 1 ms. One can clearly see the drastic change of the decay behaviors across the Feshbach resonance at 6.6 G. Well above the resonance (a), the $^1S_0$ and $^3P_2$ states have long lifetimes mainly limited by the respective one-body decay mechanism. Just above the resonance (b), both of the $^1S_0$ and $^3P_2$ states suffer from the faster decays, which should be attributed to the inelastic loss between them. When the field is swept across the resonance (c), we find the appearance of rapid loss component with the time constant of less than 30 ms both in the $^1S_0$ and $^3P_2$ states, which suggests indirectly the formation of Feshbach molecules [1]. Well below the resonance (d), the $^1S_0$ and $^3P_2$ states again show long lifetimes limited by the respective one-body decay mechanism. However, the initial atom numbers are smaller both in the $^1S_0$ and $^3P_2$ states, which suggests indirectly that the Feshbach molecules are created and are rapidly lost. This is supported by the fact that the initial atom numbers in Fig. 4(d) are almost the same as those at the values after the initial rapid decay in Fig. 4(c).

Based on the stability of states, we analyze our atom decay data with the following decay model:

$$\frac{dn_g}{dt} = -\beta_{ge} n_g n_e - \beta_{gm} n_g n_m \tag{4}$$

$$\frac{dn_e}{dt} = -\gamma_e n_e - \beta_{ge} n_g n_e - \beta_{ee} n_e^2 - \beta_{em} n_e n_m \tag{5}$$

$$\frac{dn_m}{dt} = -\beta_{gm} n_g n_m - \beta_{em} n_e n_m, \tag{6}$$

where n_g and n_e are densities of atoms in the $^1S_0$ and $^3P_2$ states, respectively, and n_m is a density of Feshbach molecules. γ_e is a one-body loss coefficient of the $^3P_2$ atoms and is fixed to 0.33 Hz. β_{ij} $(i, j = g, e, m)$ is a two-body loss coefficient of i and j components. For simplicity, we only consider two-body loss terms of $\beta_{ge} n_g n_e$, $\beta_{ee} n_e^2$, $\beta_{gm} n_g n_m$, and $\beta_{em} n_e n_m$. It is to be noted that s-wave collisions between two polarized $^3P_2$ atoms are forbidden due to Pauli principle, but a p-wave collision is possible and is taken into account. We ignore one-body and two-body decay for the $^1S_0$ atoms. In addition, we assume that only β_{ge} depends on a magnetic field, and the other loss parameters are constant.

The number of the atoms in the $^1S_0$ (N_g) and $^3P_2$ (N_e) states and the number of the molecules (N_m) are obtained by integrating Eqs. (4-6) over the whole sample,

$$\frac{dN_g}{dt} = -B_{ge} N_g N_e - B_{gm} N_g N_m \tag{7}$$

$$\frac{dN_e}{dt} = -\Gamma_e N_e - B_{ge} N_g N_e - B_{ee} N_e^2 - B_{em} N_e N_m \tag{8}$$

$$\frac{dN_m}{dt} = -B_{gm} N_g N_m - B_{em} N_e N_m, \tag{9}$$

where $(i, j = g, e, m)$

$$N_i = \iiint d\boldsymbol{r}\, n_i(\boldsymbol{r}) \tag{10}$$

$$\Gamma_i = \gamma_i \tag{11}$$

$$B_{ij} = \beta_{ij} \frac{\iiint d\boldsymbol{r}\, n_i(\boldsymbol{r}) n_j(\boldsymbol{r})}{\left[\iiint d\boldsymbol{r}\, n_i(\boldsymbol{r})\right]\left[\iiint d\boldsymbol{r}\, n_j(\boldsymbol{r})\right]}. \tag{12}$$

Now we ignore the time dependence of the parameters of Γ_i and B_{ij} and we assume that only the atom and molecule numbers N_g, N_g and N_m change. The obtained fitting parameters by use of Eqs.(7-9) are shown in Table I. The obtained value of B_{ee} = 0.14(2) mHz corresponds to β_{ee} = 1.5(2)×10^{-19} m^3/s for our typical experimental condition. This value is similar to the previously obtained loss coefficient for ultracold ^{171}Yb atoms in the F=3/2, m_F=-3/2 state [9, 30]. This is consistent with the absorption imaging result shown in Fig. 1. We note that the lifetime of Feshbach molecules of fermionic alkali atoms in a trap was reported to be about 100 ms for ^{40}K and more than one second for ^{6}Li near Feshbach resonance, where dimer-dimer relaxation is a dominant loss process [1]. The shorter lifetime of our Feshbach molecules should be attributed to the presence of the atoms, which is not removed in our current experiment.

IV. IMPLEMENTATION OF SPIN-ORBITAL COUPLING WITH A ONE-PHOTON PROCESS

Next, we describe the successful implementation of SOC with a one-photon process between the $^3P_2$ (pseudo-spin up) and ground $^1S_0$ (pseudo-spin down) states, which is another important ingredient for realizing topological superfluids. We confirm the successful implementation of SOC with several measurements.

The scheme of a two-photon Raman process is a familiar one to induce spin-orbital coupling between the hyperfine

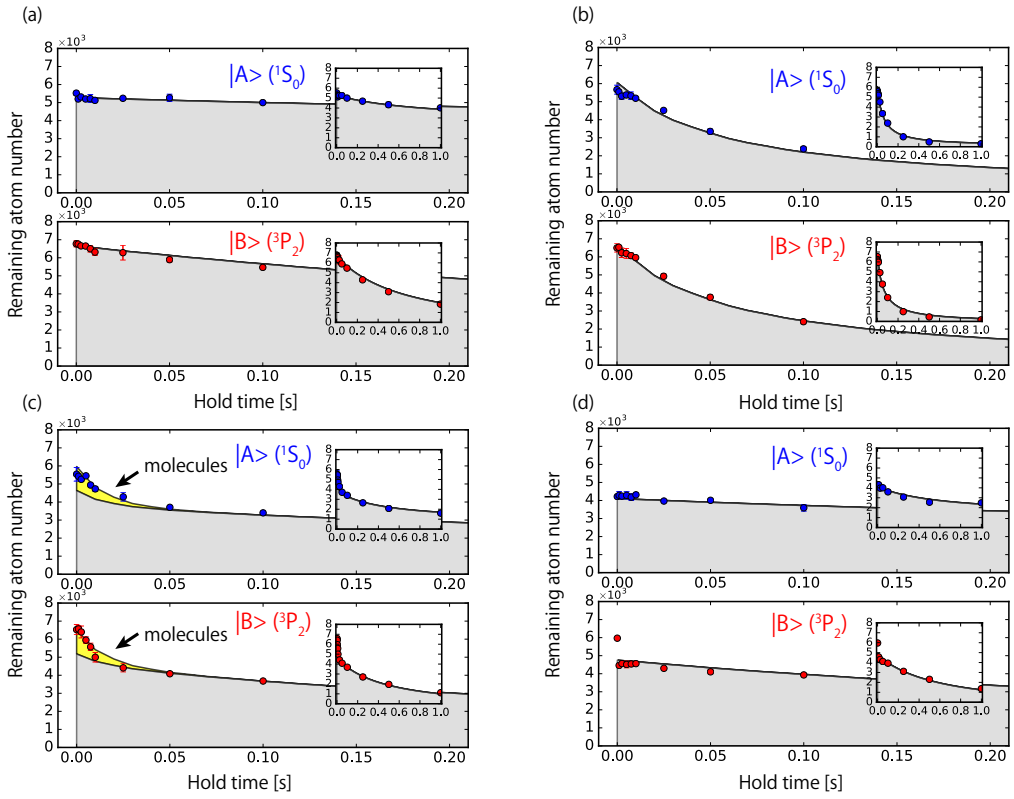

FIG. 4. Atom number in the $^1S_0$ and $^3P_2$ states as a function of the holding time after the magnetic sweep from 7.466 G to final magnetic fields of (a) 7.5 G, (b) 6.6 G, (c) 6.2 G, and (d) 5.5 G. The fitting lines are also shown. Grey (yellow) shade shows the atom (molecular) component. The fitting parameters are shown in Table I. See text for detail. The insets show the long time behaviors.

Magnetic Field [G]	$N_g(t=0)$	$N_e(t=0)$	$N_m(t=0)$	B_{ge} [mHz]	B_{ee} [mHz]	B_{gm} [mHz]	B_{em} [mHz]
5.5	$4.10(8)\times10^3$	$4.75(6)\times10^3$	0 (fixed)	0.23(3)	0.14(2)	-	-
6.2	$4.6(3)\times10^3$	$5.2(3)\times10^3$	$1.3(2)\times10^3$	0.38(8)	0.14(2)	9(4)	6(3)
6.6	$6.1(1)\times10^3$	$6.7(1)\times10^3$	0 (fixed)	2.6(2)	0.14(2)	-	-
7.5	$5.27(5)\times10^3$	$6.65(8)\times10^3$	0 (fixed)	0.08(1)	0.14(2)	-	-

TABLE I. Obtained fitting parameters. Only the data of 6.2 G are well-fitted with a non-zero molecular number at the holding time ($t = 0$). Because the data other than 6.2 G are not well fitted with a non-zero molecular number, therefore we fix the parameters $N_m(t = 0) = 0$ for the other magnetic fields. We use the same fitting value of B_{ee} for all magnetic fields.

spin states in the ground state of alkali-metal atoms. However, if we consider the electronic excited state as spin-up and the ground state as spin-down, then we can introduce a momentum transfer between these spin-up and -down states by a single-photon process [21–23], which is similarly considered as spin-orbital coupling.

A. Bosonic ^{174}Yb case

As the most basic process of the single-photon implementation of SOC, we observe a pseudo-spin flip process accompanied by a momentum transfer between the $^1S_0$ and $^3P_2$ states of cold ^{174}Yb atoms. The experimental setup and time sequence are shown in Fig. 5. Initially ^{174}Yb atoms are prepared in the ground $^1S_0$ "spin-down" state in an optical trap. Immediately after turning-off an optical trap for the measurement of momentum distributions, we apply SOC laser light near-resonant to the $^1S_0$ -$^3P_2$ transition for a 1 ms along the x direction to excite the atoms to the $^3P_2$ "spin-up" state. About 1 kHz linewidth laser for SOC at 507 nm is generated by frequency-doubling of an external-cavity laser diode at 1014 nm, locked to an ultra-low expansion cavity and slow frequency drift with a rate of about 1 kHz per hour is compensated by a frequent measurement of the $^1S_0$ -$^3P_2$ transition of ^{174}Yb atoms.

Figures 6 and 7 show the state-dependent quasi-momentum distributions for various detunings, measured by a TOF

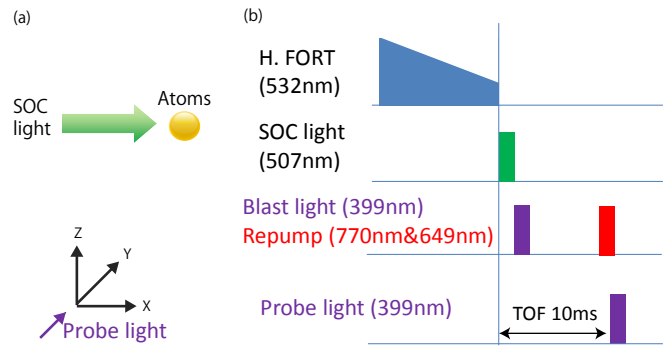

FIG. 5. (a) Experimental setup and (b) time sequence for implementation of spin-orbital coupling with a one-photon process using ^{174}Yb. See text for detail.

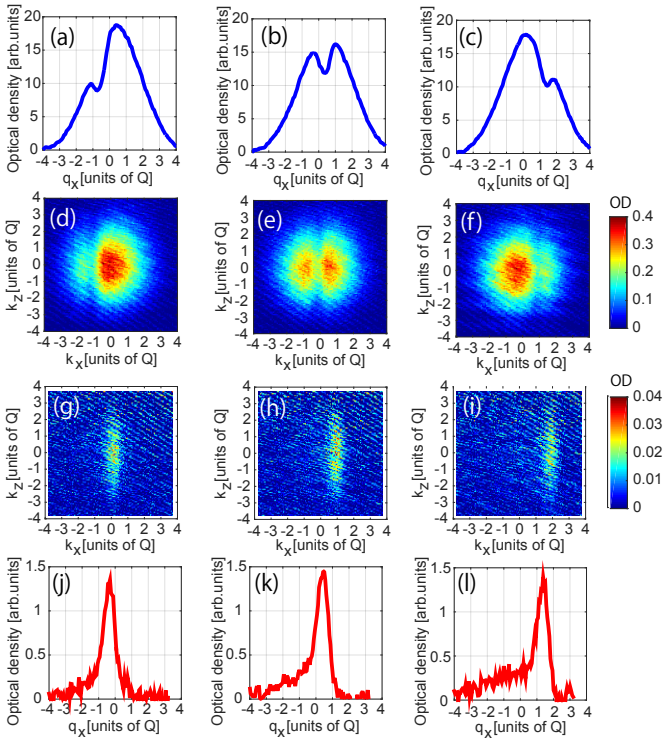

FIG. 6. Quasi-momentum distributions. (a-c) Integrated optical density for the $^1S_0$ state as a function of quasi-momentum. (d-f) atom images for the $^1S_0$ state in real momentum. (g-i) atom images for the $^3P_2$ state in real momentum. (j-l) Integrated optical density for the $^3P_2$ state as a function of quasi-momentum.(a, d, g, j) -8 kHz detuning. (b, e, h, k) 0 kHz detuning. (c, f, i, l) +8 kHz detuning.

method. Here we define a quasi-momentum q_x=k_x + $\sigma_z Q/2$ where σ_z=+1(−1) for atoms in the $^1S_0$ ($^3P_2$) state and a recoil momentum Q from SOC light propagating along the x axis, is given by h/λ, in which λ is the wavelength of SOC light and k_x is a real momentum. In order to observe the quasi-momentum distributions of the $^3P_2$ state, first we remove the $^1S_0$ atoms by blast light resonant to the $^1S_0$ -$^1P_1$ transition at the start of the TOF time (10 ms), then transfer the atoms from the $^3P_2$ to

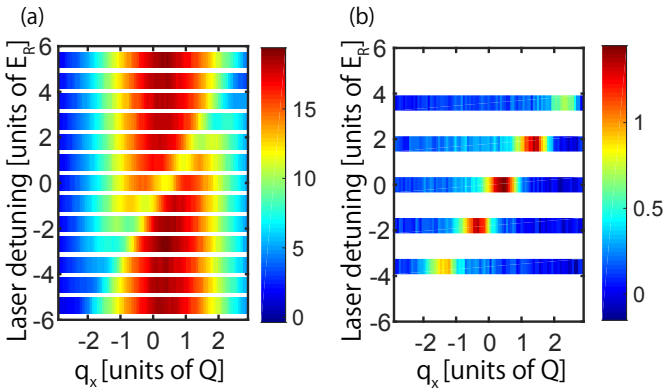

FIG. 7. Quasi-momentum distributions of integrated optical density, which are obtained by integrating the optical densities along the z axis, as a function of laser detuning in the (a) $^1S_0$ and (b) $^3P_2$ states.

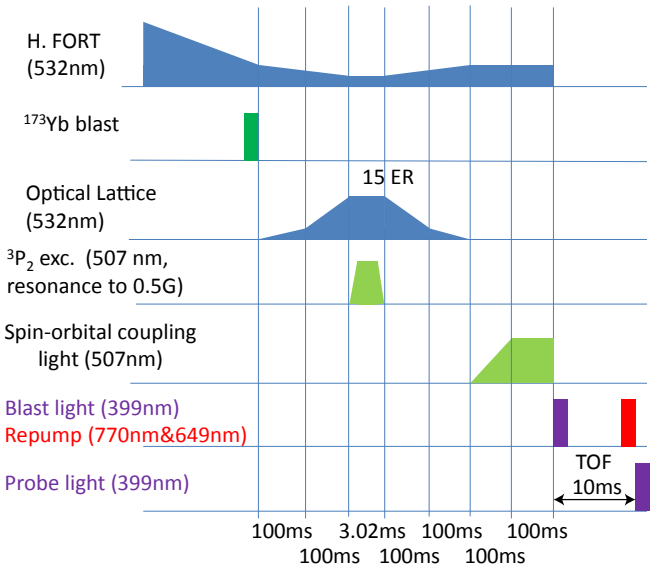

FIG. 8. Time sequence for implementation of spin-orbital coupling with a one-photon process using ^{171}Yb. See text for detail.

$^1S_0$ state by use of repumping light of about 1 ms at the end of the TOF time, and finally detected the atoms with absorption imaging. It is clear that each peak in the quasi-momentum distribution of the $^3P_2$ state coincide with the corresponding dip in the $^1S_0$ state quasi-momentum distribution.

B. Fermionic ^{171}Yb case

Next, we describe the successful implementation of SOC with a one-photon process for fermionic ^{171}Yb atoms between the $^3P_2$ ($|B\rangle$, pseudo-spin up) and ground $^1S_0$ ($|C\rangle$, pseudo-spin down) states. Here we measure state-dependent quasi-momentum distributions of fermionic ^{171}Yb atoms by use of an absorption imaging method. The time sequence is shown in Fig. 8. Initially sympathetic evaporative cooling is performed

with a single component of ^{173}Yb and a single component ^{171}Yb in the $|C\rangle$ state to suppress a three-body recombination loss, resulting in the typical temperature of 30 nK with about 10^4 atoms corresponding to 0.2 T_F and the atom density of $2 \times 10^{13}/\mathrm{cm}^3$. Note that we experimentally determine the Rabi frequency Ω of the $^1S_0$ -$^3P_2$ transition by observing a Rabi oscillation. At an intensity of 4.2 W/cm^2, it is measured to be $2\pi \times 4.4$ kHz, corresponding to 0.98 E_R, where E_R is the photon recoil energy of 507-nm light. We confirm that the Rabi oscillation is damped in 2 ms during the excitation in the optical lattice, probably due to inhomogeneity, and therefore we adopt the excitation time of 3 ms for preparation of incoherent spin mixture of ^{171}Yb atoms in the $|C\rangle$ and $|B\rangle$ states. After we excite half of the atoms in the $|C\rangle$ state into the $|B\rangle$ state at 0.5 G, we decrease the lattice depth from 15 E_R to zero in 200 ms. After turning off the optical lattice, SOC light is introduced, the intensity of which linearly increases from zero to a final value up to about 6 E_R, while the laser frequency is kept constant. Note that the laser source of SOC light is the same as the laser for the $|C\rangle + |B\rangle$ mixture preparation, but the frequency is independently controlled.

An optical trap as well as SOC light are suddenly turned off, and we measure momentum distributions with a 10 ms TOF time in a similar procedure to that of a momentum transfer measurement. Figure 9 (a) show the atom distribution as a function of a quasi-momentum, in which the SOC light propagates along the x axis (see also Fig. 9 (b)).

The energy dispersion are obtain by diagonalizing an effective single particle Hamiltonian as a function of quasi-momentum $\mathbf{q}=(q_x, q_y = k_y, q_z = k_z)$

$$H = \begin{pmatrix} \frac{1}{2m}\left(q_x - \frac{Q}{2}\right)^2 & \frac{\hbar\Omega}{2} \\ \frac{\hbar\Omega}{2} & \frac{1}{2m}\left(q_x + \frac{Q}{2}\right)^2 \end{pmatrix} + \frac{q_y^2}{2m} + \frac{q_z^2}{2m}, \qquad (13)$$

where $\hbar$ is the Planck constant divided by 2π. The two energy eigenvalues E_+ and E_- of the eigenstates $|+\rangle$ and $|-\rangle$ of the Hamiltonian are obtained as

$$E_\pm(\mathbf{q}) = \sum_{i=x,y,z} \frac{q_i^2}{2m} + \frac{E_R}{4} \pm \sqrt{\left(\frac{\hbar\Omega}{2}\right)^2 + \left(\frac{Qq_x}{2m}\right)^2}, \qquad (14)$$

respectively [18, 23]. (see also Fig. 9(d-g)). Under the assumption of the Gaussian distribution, the atom densities of each branches $|\pm\rangle$ are

$$n_\pm(\mathbf{q}) = \int \frac{d\mathbf{r}}{(2\pi\hbar)^3} \exp \frac{\mu - E_\pm(\mathbf{q}) - V(\mathbf{r})}{k_B T}, \qquad (15)$$

where k_B is the Boltzmann constant, $V(r)$ is a trap potential, μ is a chemical potential, T is an atom temperature.

For simplicity we consider the linear distribution of the atoms, which is obtained by integrating along the y and z directions. The experimentally observable atom density distributions are the ones of the $^1S_0$ component $n_{^1S_0}(k_x)$ and the $^3P_2$ component $n_{^3P_2}(k_x)$ as functions of real momenta, not the spin-orbital-coupled distributions of $n_+(q_x)$ and $n_-(q_x)$. From the eigenstates of the Hamiltonian we obtain the following relations between them,

$$n_{^1S_0}\left(k_x = q_x - \frac{Q}{2}\right) = u_{q_x}^2 n_+(q_x) + v_{q_x}^2 n_-(q_x), \qquad (16)$$

$$n_{^3P_2}\left(k_x = q_x + \frac{Q}{2}\right) = v_{q_x}^2 n_+(q_x) + u_{q_x}^2 n_-(q_x), \qquad (17)$$

where $u_{q_x}^2$ and $v_{q_x}^2$ are [18]

$$u_{q_x}^2 = \frac{1}{2}\left[1 - \frac{Qq_x/2m}{\sqrt{\left(\frac{\hbar\Omega}{2}\right)^2 + \left(\frac{Qq_x}{2m}\right)^2}}\right], \qquad (18)$$

$$v_{q_x}^2 = \frac{1}{2}\left[1 + \frac{Qq_x/2m}{\sqrt{\left(\frac{\hbar\Omega}{2}\right)^2 + \left(\frac{Qq_x}{2m}\right)^2}}\right]. \qquad (19)$$

For Ω=0, $u_{q_x}^2$=0 and $v_{q_x}^2$=1, so the momentum distributions $n_{^1S_0}(q_x - Q/2)$ and $n_{^3P_2}(q_x + Q/2)$ correspond to those of $n_-(q_x)$ and $n_+(q_x)$, respectively. However, $u_{q_x}^2$=$v_{q_x}^2$=1/2 for large enough Ω, then the momentum distributions are considerably mixed and altered.

The center-of-mass position of an atom cloud, obtained by fitting the distribution of $n_{^1S_0}$ and $n_{^3P_2}$ using a Gaussian function, is shown in Fig. 9 (c). Without SOC light, the states with the spin-down ($|C\rangle$) and -up ($|B\rangle$) have quasi-momenta of $+Q/2$ and $-Q/2$, respectively. This means that the real momentum is almost zero, irrespective of the spin-up or -down. However, as a Rabi frequency increases, more atoms are concentrating around zero quasi-momentum. Namely, the real momenta take the values of almost $-Q/2$ and $+Q/2$ for spin-down and -up, respectively. This behavior indicates that the spin and the real momentum are correlated, which is called spin-momentum locking. The solid line shows a theoretically calculated center-of-mass position of an atom cloud under an assumption of Gaussian atom distribution and the temperature of 150 nK, which shows an agreement with the experimental data. In Fig. 9 (d)-(g), we show the energy dispersions for four different values of Rabi-frequencies corresponding to the experiments in Fig.9 (a) and (c). The calculations are consistent with the behaviors observed in Fig. 9 (c).

V. CONCLUSION

In conclusion, we successfully associate Feshbach molecules $^{171}Yb_2$ in the metastable state from atoms in the $^1S_0$ and $^3P_2$ states by sweeping a magnetic field across the Feshbach resonance, confirmed by a direct absorption imaging with a Stern-Gerlach separation separation. The atom loss measurement using a MOT is well explained by our decay model which takes into consideration the formation of the Feshbach molecules. The atom temperature before association is 0.37 T_F, and the optimized molecular conversion probability is 54 %, which is consistent with the theory. In addition, we successfully implement SOC with a one-photon process between the $^3P_2$ (pseudo-spin up) and $^1S_0$ (pseudo-spin down) states of ^{171}Yb, confirmed by observing a pseudo-spin flip process accompanied by a momentum transfer and a spin-momentum locking at a large Rabi frequency. The successful production of Feshbach molecules, along with the demonstrated implementation of SOC between the $^1S_0$ and $^3P_2$ states for this system, provides an important step towards p-wave topological superfluids.

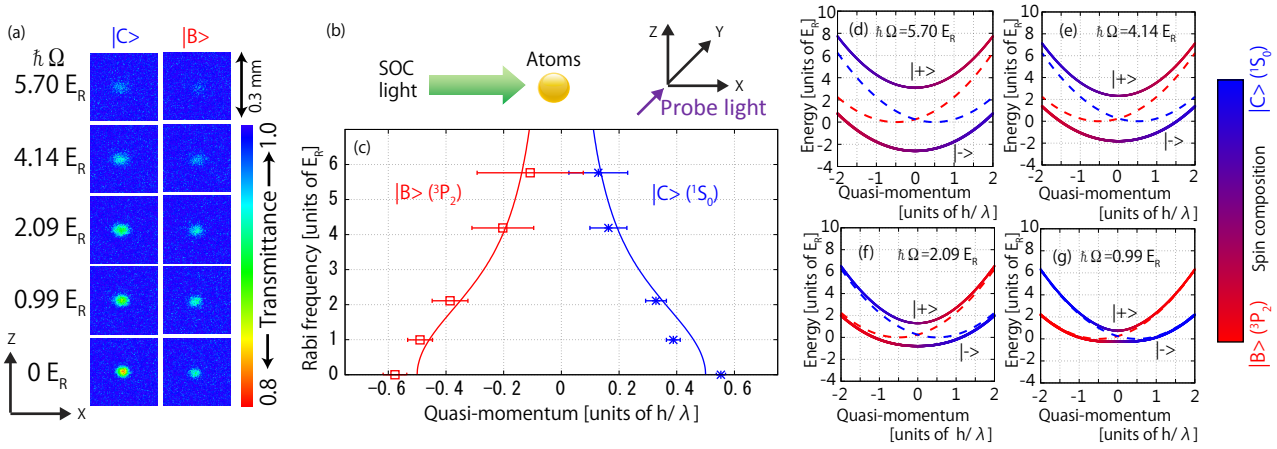

FIG. 9. Spin-momentum locking. (a) Absorption images of the $^1S_0$ ($|C\rangle$) and $^3P_2$ ($|B\rangle$) states for various Rabi frequencies (b) Schematic view of the experimental configuration. (c) Center-of-mass positions of an atom cloud of $|C\rangle$ (asterisk, blue) and $|B\rangle$ (open box, red), obtained by fitting using a Gaussian function. Solid lines with blue and red are the theoretically calculated center-of-mass position of an atom cloud for $|C\rangle$ and $|B\rangle$, respectively, under the assumptions of a Gaussian function for the atom distribution and 150 nK for the atom temperature. (d-g) Energy dispersions. See the text for details. The solid lines correspond to $E_\pm$ in the presence of SOC and dotted lines are those without SOC. The colors of red and blue indicate the compositions of $|B\rangle$ and $|C\rangle$ states, respectively.

ACKNOWLEDGMENTS

We thank J. Sakamoto for experimental assistance. This work is supported by MEXT/JSPS KAKENHI Grant Numbers JP25220711, JP26247064, JP16H00990, JP16H01053, JP16H00801, and CREST, JST JPMJCR 1673, and Matsuo Foundation.

[1] T. Köhler, K. Góral, and P. S. Julienne, Rev. Mod. Phys. **78**, 1311 (2006).

[2] C. A. Regal, M. Greiner, and D. S. Jin, Phys. Rev. Lett. **92**, 040403 (2004).

[3] M. W. Zwierlein, J. R. Abo-Shaeer, A. Schirotzek, C. H. Schunck, and W. Ketterle, Nature **435**, 1047 (2005).

[4] J. M. Sage, S. Sainis, T. Bergeman, and D. DeMille, Phys. Rev. Lett. **94**, 203001 (2005).

[5] J. G. Danzl, E. Haller, M. Gustavsson, M. J. Mark, R. Hart, N. Bouloufa, O. Dulieu, H. Ritsch, and H.-C. Nägerl, Science **321**, 1062 (2008).

[6] K.-K. Ni, S. Ospelkaus, M. H. G. de Miranda, A. Pe'er, B. Neyenhuis, J. J. Zirbel, S. Kotochigova, P. S. Julienne, D. S. Jin, and J. Ye, Science **322**, 231 (2008).

[7] S. A. Moses, J. P. Covey, M. T. Miecnikowski, B. Yan, B. Gadway, J. Ye, and D. S. Jin, Science **350**, 659 (2015).

[8] S. Kato, R. Yamazaki, K. Shibata, R. Yamamoto, H. Yamada, and Y. Takahashi, Phys. Rev. A **86**, 043411 (2012).

[9] S. Taie, S. Watanabe, T. Ichinose, and Y. Takahashi, Phys. Rev. Lett. **116**, 043202 (2016).

[10] R. Zhang, Y. Cheng, H. Zhai, and P. Zhang, Phys. Rev. Lett. **115**, 135301 (2015).

[11] G. Pagano, M. Mancini, G. Cappellini, L. Livi, C. Sias, J. Catani, M. Inguscio, and L. Fallani, Phys. Rev. Lett. **115**, 265301 (2015).

[12] M. Höfer, L. Riegger, F. Scazza, C. Hofrichter, D. R. Fernandes, M. M. Parish, J. Levinsen, I. Bloch, and S. Fölling, Phys. Rev. Lett. **115**, 265302 (2015).

[13] C. Chin, R. Grimm, P. Julienne, and E. Tiesinga, Rev. Mod. Phys. **82**, 1225 (2010).

[14] M. Z. Hasan and C. L. Kane, Rev. Mod. Phys. **82**, 3045 (2010).

[15] J. Dalibard, F. Gerbier, G. Juzeliūnas, and P. Öhberg, Rev. Mod. Phys. **83**, 1523 (2011).

[16] M. Sato, Y. Takahashi, and S. Fujimoto, Phys. Rev. Lett. **103**, 020401 (2009).

[17] X.-J. Liu and H. Hu, Phys. Rev. A **85**, 033622 (2012).

[18] P. Wang, Z.-Q. Yu, Z. Fu, J. Miao, L. Huang, S. Chai, H. Zhai, and J. Zhang, Phys. Rev. Lett. **109**, 095301 (2012).

[19] L. W. Cheuk, A. T. Sommer, Z. Hadzibabic, T. Yefsah, W. S. Bakr, and M. W. Zwierlein, Phys. Rev. Lett. **109**, 095302 (2012).

[20] N. Q. Burdick, Y. Tang, and B. L. Lev, Phys. Rev. X **6**, 031022 (2016).

[21] M. L. Wall, A. P. Koller, S. Li, X. Zhang, N. R. Cooper, J. Ye, and A. M. Rey, Phys. Rev. Lett. **116**, 035301 (2016).

[22] M. Mancini, G. Pagano, G. Cappellini, L. Livi, M. Rider, J. Catani, C. Sias, P. Zoller, M. Inguscio, M. Dalmonte, and L. Fallani, Science **349**, 1510 (2015).

[23] Z. Qi, G. Jiang-Bin, and O. Choo-Hiap, Chinese Physics Letters **30**, 080301 (2013).

[24] B. Song, C. He, S. Zhang, E. Hajiyev, W. Huang, X.-J. Liu, and G.-B. Jo, Phys. Rev. A **94**, 061604 (2016).

[25] S. Taie, Y. Takasu, S. Sugawa, R. Yamazaki, T. Tsujimoto, R. Murakami, and Y. Takahashi, Phys. Rev. Lett. **105**, 190401 (2010).

[26] For review, A. Tannús and M. Garwood, NMR in Biomedicine **10**, 423 (1997).

[27] E. Hodby, S. T. Thompson, C. A. Regal, M. Greiner, A. C. Wilson, D. S. Jin, E. A. Cornell, and C. E. Wieman, Phys. Rev. Lett. **94**, 120402 (2005).

[28] W. Ketterle and M. W. Zwierlein, Rivista Del Nuovo Cimento **31**, 247 (2008), arXiv:0801.2500.

[29] E. Timmermans, Phys. Rev. Lett. **87**, 240403 (2001).

[30] S. Watanabe, S. Taie, and Y. Takahashi, unpublished.